Appendix

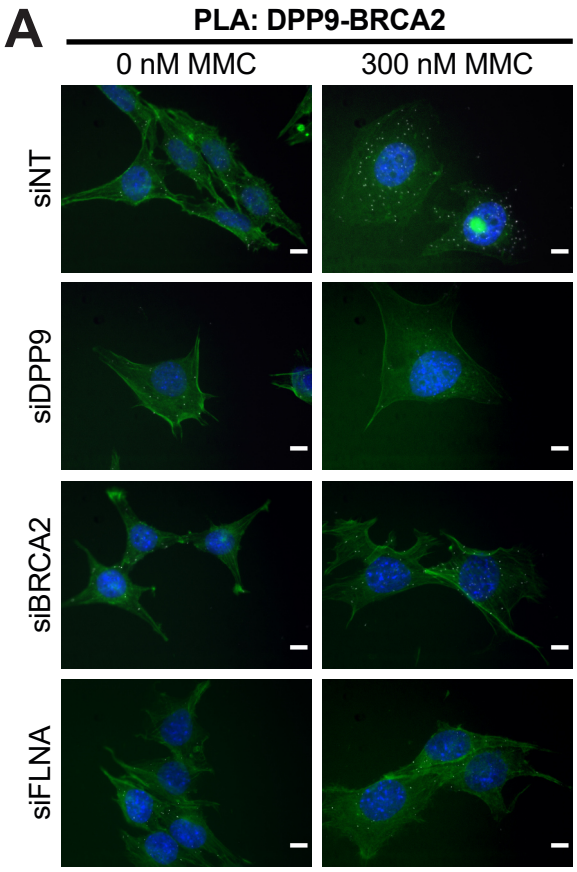

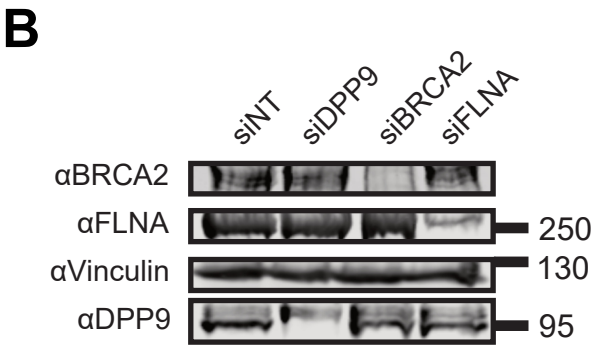

Appendix Figure S1

Appendix Figure S1: DPP9-BRCA2 PLA images

A. Representative PLA images showing close proximity between endogenous DPP9 and endogenous BRCA2 in HeLa WT cells. Exposure of cells to MMC triggers more PLA events. Phalloidin (green) stains actin filaments, DAPI (blue) stains the nucleus. Scale bar 10 μm. Anti-BRCA2: RRID:AB_2259370, Anti-DPP9: RRID:AB_2889071.

B. Representative Western Blot showing the silencing efficiency of HeLa WT cells (A) for DPP9 (siDPP9), BRCA2 (siBRCA2), FLNA (siFLNA) with respect to not-targetted controls (siNT). Vinculin was used as a loading control. Anti-BRCA2: RRID:AB_2259370, Anti-FLNA: RRID:AB_877728, Anti-Vinculin: RRID:AB_477629, Anti-DPP9: RRID:AB_2889071.

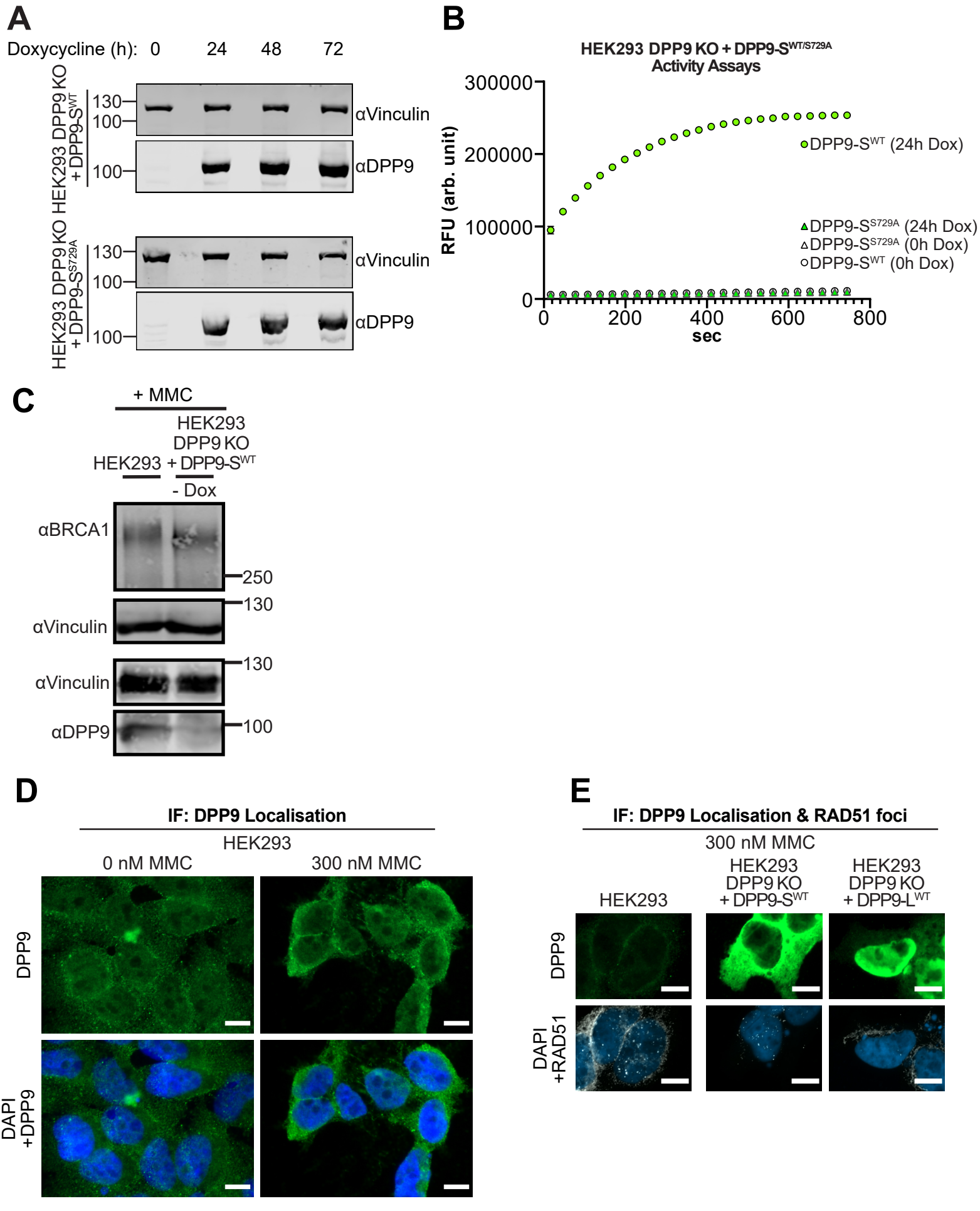

Appendix Figure S2

Appendix Figure S2: Characterization of DPP9 variants in the HEK293 DPP9 KO background

A. Western Blot, showing the time-dependent doxycycline induced expression of DPP9-S^{WT} or DPP9-S^{S729A} in HEK293 DPP9 KO + DPP9-S^{WT} and HEK293 DPP9 KO + DPP9-S^{S729A} cells. Vinculin was a loading control.

B. Graph showing DPP9 activity in cell lysates following a 24 h incubation with Doxycycline for expression of DPP9-S^{WT} in HEK293 DPP9 KO + DPP9-S^{WT}, or the enzymatically inactive DPP9-S^{S729A} in HEK293 DPP9 KO + DPP9-S^{S729A} cells. Cell lysates were prepared following 24 h of exposure to Doxycycline and tested for activity against an artificial DPP9 substrate Gly-Pro-7-amido-4-methylcoumarin hydrobromide (GP-AMC), showing DPP9 activity in cells induced for the expression of the DPP9-S^{WT} but not of DPP9-SS729A.

C. Representative Western Blots showing the levels of DPP9 and BRCA1 in HEK293 and HEK293 DPP9 KO + DPP9-S^{WT} cells without Doxycycline treatment. Vinculin was a loading control. Anti-BRCA1: RRID:AB_626761, anti-DPP9: RRID:AB_731947, anti-Vinculin: RRID:AB_477629.

D. Immunofluorescence images showing a cytosolic and nuclear localization of DPP9 in HEK293 cells in the presence and absence of MMC induction. DPP9 is shown in green, nuclei (DAPI) are shown in blue. Scale bar 10 µm. Anti-DPP9: RRID:AB_2889071.

E. Immunofluorescence images showing the overexpression levels and localization of the DPP9-S^{WT} and DPP9-L^{WT} in HEK293 DPP9 KO + DPP9-S^{WT} and HEK293 DPP9 KO + DPP9-L^{WT} cells in the presence of MMC-induced DNA Damage. DPP9 is shown in green, RAD51 in white, nuclei (DAPI) are shown in blue. Scale bar 10 µm. Anti-DPP9: RRID:AB_2889071, Anti-RAD51: RRID:AB_1142428.

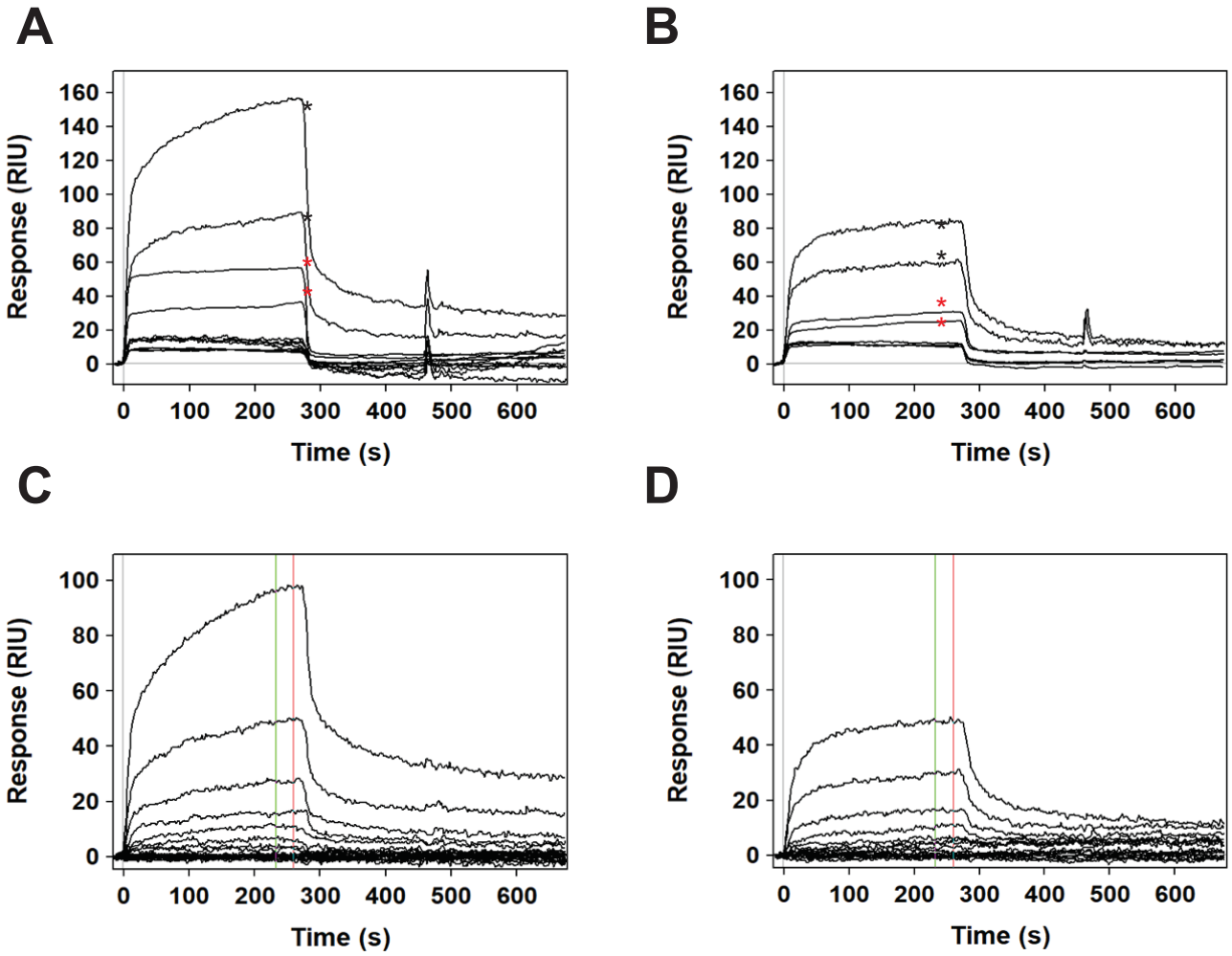

Appendix Figure S3

Appendix Figure S3: DPP9 binds directly to the BRCA2 N-terminal peptides

A. Sensograms obtained for interactions observed between DPP9 (ligand) and $BRCA2_{1-40}$ (analyte). Displayed are raw data before referencing. Marked by (*black) are sensograms obtained for interactions between ligand and analyte recorded on the ligand channel. Marked by (*red) are sensograms obtained for interactions between ligand and analyte recorded on the reference channel. Sensograms displayed are a representative of three independent measurements, each containing three technical replicates. Data analyses was performed with Scubber 2.0c, sensograms were double referenced and equilibrium binding response data exported and further analysed by GraphPad Prism.

B. Analogous to (A), Ligand DPP9 and Analyte $BRCA2_{3-40}$. Shown are raw data before referencing.

C. Sensogram obtained for a serial dilution of $BRCA2_{1-40}$ (analyte) injected over a surface, on which 800-1000 RIU DPP9 (ligand) were immobilized. For each analyte injection two buffer injections were performed. Data was double referenced (1st: reference channel, 2nd: buffer injections).

D. Sensogram obtained for a serial dilution of $BRCA2_{3-40}$ (analyte) injected over a surface, on which 800-1000 RIU DPP9 (ligand) were immobilized, as described in (C)**.**

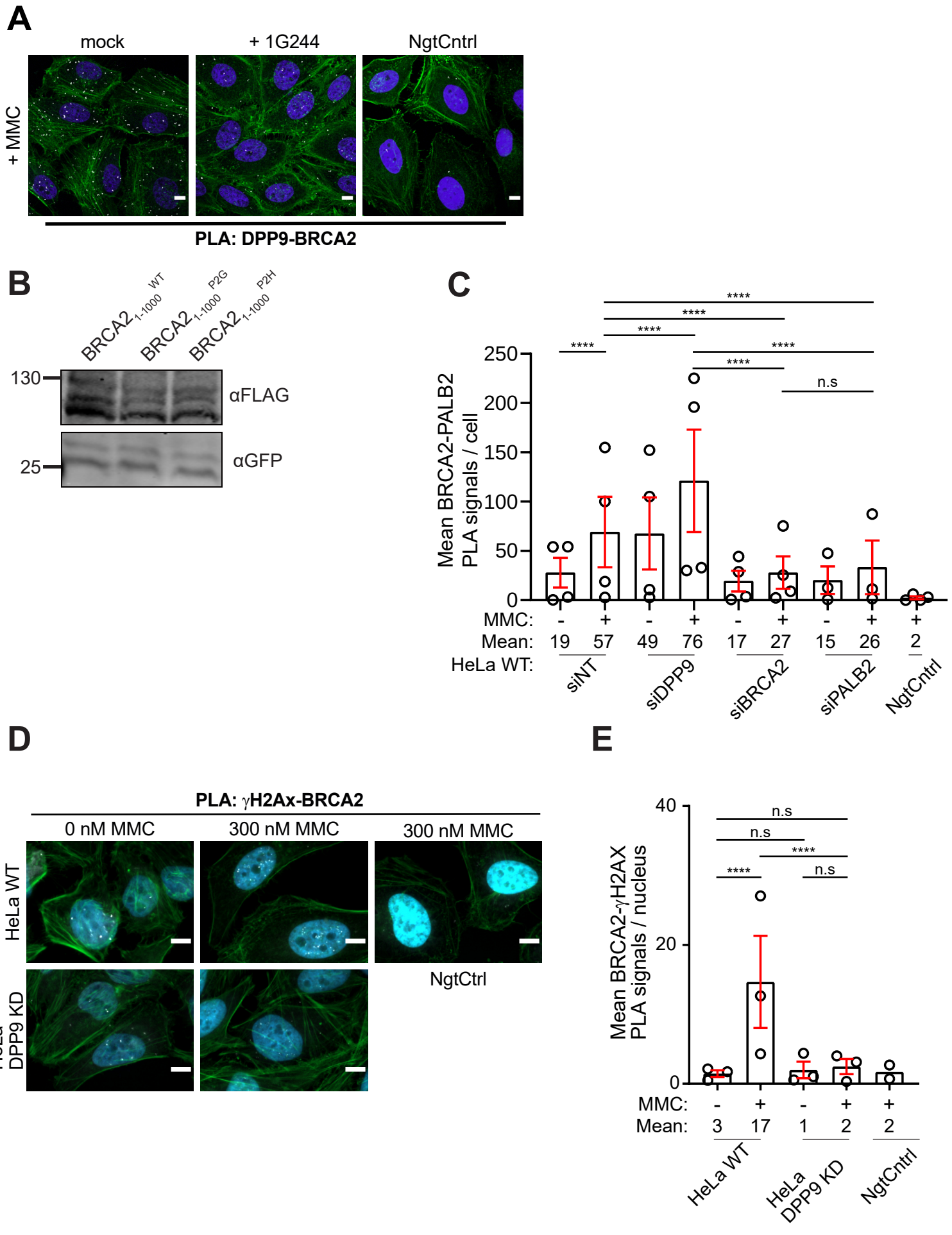

Appendix Figure S4

Appendix Figure S4: Western blots and summary of PLA experiments between BRCA2 and DPP9, BRCA2 and PALB2 and, BRCA2 and γH2AX

A. Representative images of HeLa WT cells, showing DPP9-BRCA2 PLA (white) in the presence of 1G244 – a competitive inhibitor of DPP9. Control cells were mock treated with DMSO. Phalloidin (green) stains actin filaments, DAPI (blue) stains the nucleus. Scale bar 10 μm. Anti-BRCA2: RRID:AB_2259370, Anti-DPP9: RRID:AB_2889071.

B. Western Blot image showing the steady state levels of C-terminally FLAG-tagged $BRCA2_{1\text{-}1000}^{WT}$, $BRCA2_{1\text{-}1000}^{P2G}$ and $BRCA2_{1\text{-}1000}^{P2H}$ fragments. The steady state levels of the $BRCA2_{1\text{-}1000}^{P2G}$ and $BRCA2_{1\text{-}1000}^{P2H}$ constructs are lower than those of $BRCA2_{1\text{-}1000}$ implying that the proline in the second position is a determining factor of $BRCA2_{1\text{-}1000}$ fragment stability. GFP was used as a transfection control. Anti-FLAG: RRID:AB_262044, Anti-GFP: RRID:AB_641123.

C. Summary of PLAs between BRCA2 and PALB2 in HeLa WT cells treated with non-targeting siRNA (siNT) or silenced with the indicated oligos. Each dot represents the mean number of PLA events in a single repetition, from three to four biological replicates. More than 100 cells were quantified per condition in each experiment. Data from the summary of all PLA events per cell were analysed by a two-way ANOVA, with Tukey's Multiple Comparison test. Shown are Mean ± SEM. (**** = $p \leq 0.0001$).

D. Representative PLA images of HeLa WT and HeLa DPP9 KD cells. Fewer γH2Ax-BRCA2 PLA events (white) in HeLa DPP9 KD cells. Phalloidin (green) stains actin filaments, DAPI (blue) stains the nucleus. Scale bar 10 μm. Anti-γH2Ax: RRID:AB_2118009, Anti-BRCA2: RRID:AB_2259370.

E. Summary of PLAs between BRCA2 and γH2Ax in HeLa WT and HeLa DPP9 KD cells. Each dot represents the mean number of PLA events in a single repetition, from three biological replicates. More than 100 cells were quantified per condition in each experiment. Data from the summary of all PLA events per cell were analysed by a two-way ANOVA, with Tukey's Multiple Comparison test. Shown are Mean ± SEM. (**** = $p \leq 0.0001$).

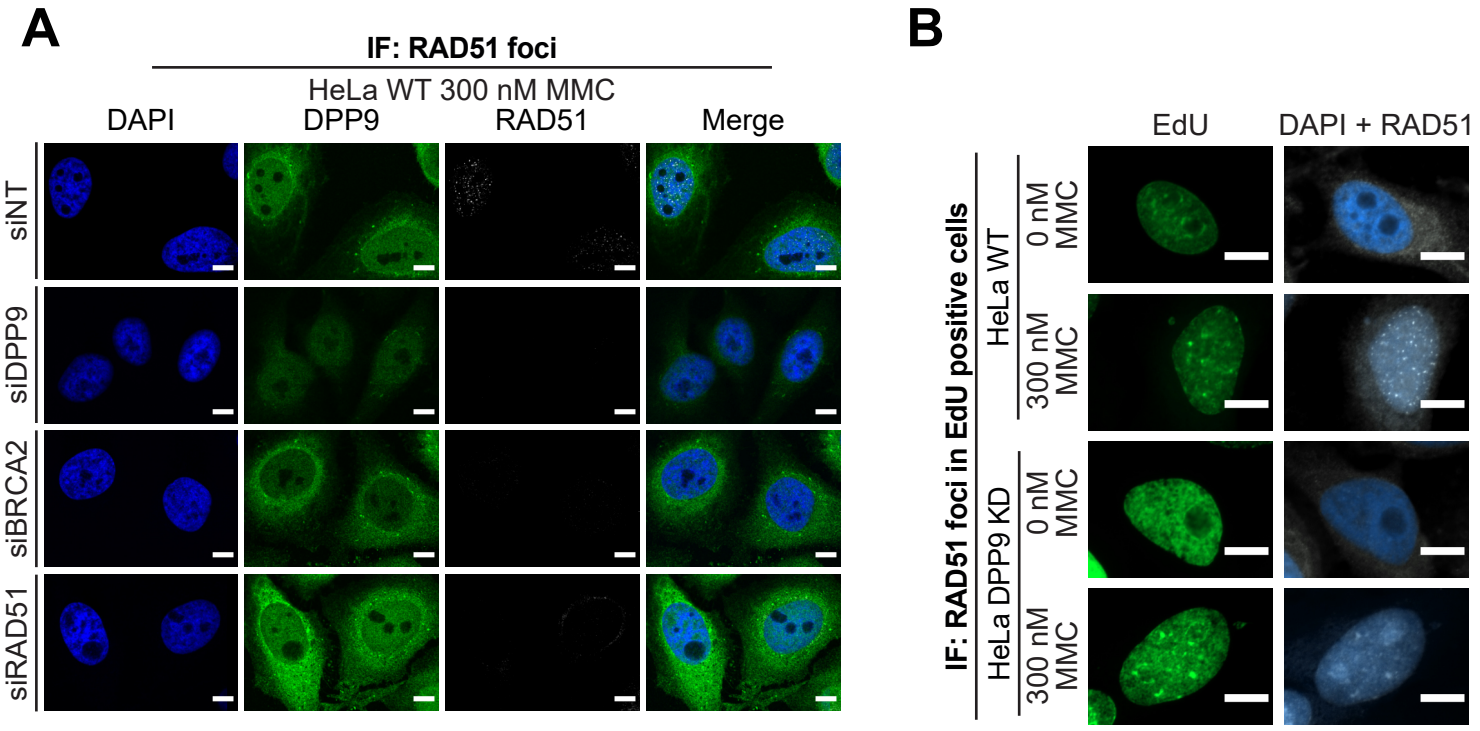

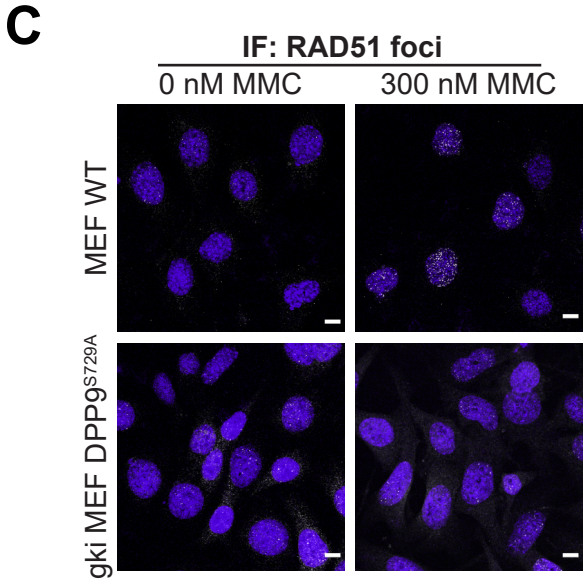

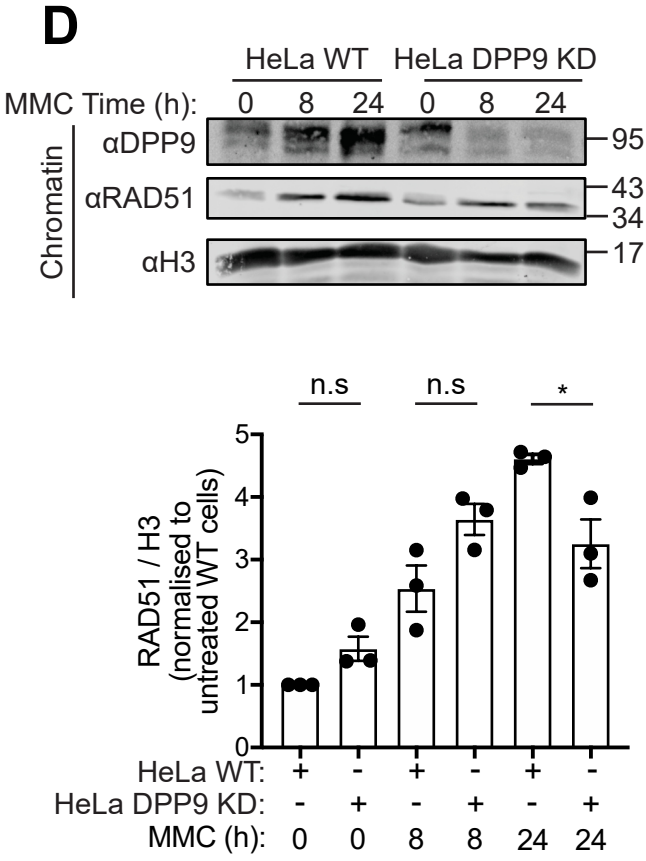

Appendix Figure S5

Appendix Figure S5: DPP9 activity promotes RAD51 foci formation and chromosomal association

A. Representative immunofluorescence images showing fewer MMC-induced RAD51 foci (white, RRID:AB_1142428) in HeLa WT cells silenced for DPP9 (siDPP9) compared to HeLa WT cells targeted with non-coding siRNA (siNT). Control cells were silenced for BRCA2 (siBRCA2) or RAD51 (siRAD51). DPP9 is shown in green, nuclei (DAPI) are shown in blue. Scale bar 10 μm. Anti-DPP9: RRID:AB_2889071, Anti-RAD51: RRID:AB_1142428.

B. Representative immunofluorescence images showing fewer RAD51 foci (white, RRID:AB_1142428) in EdU positive (green) HeLa DPP9 KD cells. DAPI (blue) stains the nucleus. Scale bar 10 μm. Anti-RAD51: RRID:AB_1142428.

C. Immunofluorescence images revealing fewer RAD51 foci (white) in gki MEF DPP9^{S729A} cells expressing inactive DPP9, compared to MEF WT cells, following exposure to MMC. Nuclei (DAPI) are shown in blue. Scale bar 10 μm. Anti-RAD51: RRID:AB_1142428.

D. Representative Western Blot images and quantification of three biological replicates showing that following 24 h incubation with MMC, less RAD51 is associated with chromatin in HeLa DPP9 KD cells compared to HeLa WT cells. Histone 3 (RRID:AB_331563) was a loading control. Quantification was normalised to HeLa WT cells in the absence of MMC. Data were analysed by a two-way ANOVA with Tukey's Multiple Comparison test. Shown are Mean ± SEM. (* = $p \leq 0.05$).

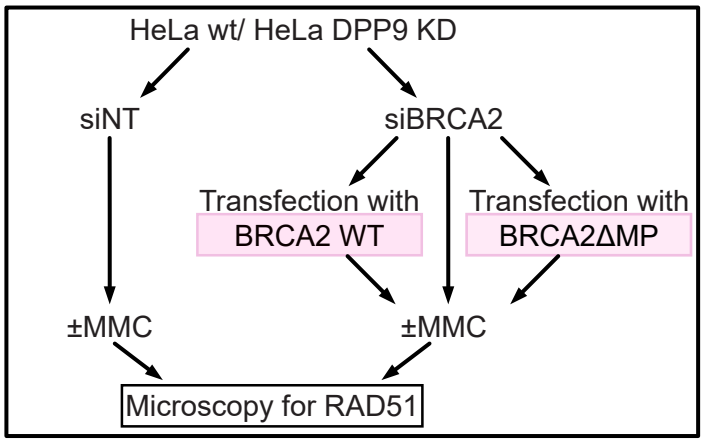

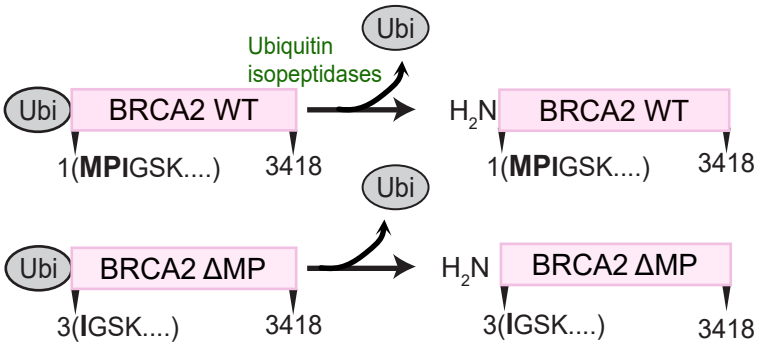

Appendix Figure S6

Appendix Figure S6: Experimental setup for RAD51 foci rescue assay

Experimental setup for HeLa WT and HeLa DPP9 KD cells silenced for endogenous BRCA2 and transfected with full-length $BRCA2_{1-3418}$ or $BRCA2\Delta MP_{3-3418}$ constructs and graphical presentation of the full-length $BRCA2_{1-3418}$ and $BRCA2\Delta MP_{3-3418}$ constructs. Cells that are transiently silenced for BRCA2 (siBRCA2) are pooled and split into 3 groups (siBRCA2, siBRCA2 + BRCA2 WT_{1-3418}, siBRCA2ΔMP_{3-3418}). Both BRCA2 variants are fused to an N-terminal ubiquitin tag, which is removed in cells by endogenous ubiquitin-proteases to expose the desired, defined N-terminus.

Appendix Table S1: Crystallographic table

Table. Crystallographic parameters for DPP8 and DPP9 -BRCA2 -peptide structures.

	DPP8 - BRCA2 peptide	DPP9 - BRCA2 peptide
Data Collection		
Space Group	$C222_1$	$P2_12_12_1$
Resolution (Å)	44.58-3.20 (3.28-3.20)[a]	43.47-3.00 (3.19-3.00)[a]
Cell dimensions		
a, b, c (Å)	162.73 246.07 261.81	119.53 117.32 163.42
α, β, γ (Å)	90, 90, 90	90, 105.74, 90
R-merge	13.4 (131.4)[a]	13.1(30.7)[a]
I/σ	17.2 (1.8)[a]	5.9(3.0)[a]
Completeness (%)	99.9 (99.2)[a]	87.8(88.8)[a]
Redundancy	8.37 (8.34)[a]	2.65(2.53)[a]
Total observations	725357 (52815)[a]	202589(33069)[a]
Total unique observations	86559 (6331)[a]	76534(13092)[a]
Refinement		
R_{cryst}/R_{free}	18.39/22.47	28.5/34.5
Number of reflections	82126 (4323)[b]	72706(3827)[b]
RMS bonds (°)	0.003	0.004
RMS angles (°)	0.984	1.120
Number of atoms	20409	26316
Average B-factor	84.8	25.5
Ramachandran plot (%)		
Preferred region	2312	2904
Allowed region	147	228
Outliers	16	27

[a] Values in parentheses correspond to the highest-resolution shell
[b] Values in parentheses correspond to free R-value test set